Detailed Numerical Simulation of Cathode Spots in Vacuum Arcs—I

Mário D. Cunha, Helena T. C. Kaufmann, Mikhail S. Benilov, Werner Hartmann, and Norbert Wenzel

***Abstract*— A model of cathode spots in high-current vacuum arcs is developed, with account of the plasma cloud left over from a previously existing spot, all mechanisms of current transfer to the cathode surface, including the contribution of the plasma produced by ionization of the metal vapor emitted in the spot, and the Joule heat generation in the cathode body. The simulation results allow one to clearly identify the different phases of life of an individual spot: the ignition, the expansion over the cathode surface, and the thermal explosion. The expansion phase is associated with a nearly constant maximum temperature of the cathode, which occurs at the surface and is approximately 4700–4800 K. Thermal explosion is a result of thermal instability (runaway), which develops below the cathode surface when the Joule heating comes into play. The development of the spot is interrupted if the plasma cloud has been extinguished: the spot is destroyed by heat removal into the bulk of the cathode due to thermal conduction. Therefore, different scenarios are possible depending on the time of action of the cloud: the spot may be quenched before having been formed or during the expansion phase, or even at the initial stage of thermal explosion.**

***Index Terms*— Arc discharges, electrodes, vacuum arcs.**

I. Introduction

EROSION of cathode material in vacuum arcs provides the medium for the discharge, the cathode vapor, and the understanding of the plasma–cathode interaction is one of the most important issues in the theory of vacuum arcs. In some cases, current transfer to cathodes of vacuum arcs can occur in the diffuse mode. [This happens when the average temperature of the cathode surface is high enough, typically around 2000 K (see [1] and the references therein). It is interesting to note that the physics of this regime, while supposedly being relatively simple, still has not been fully understood (see [2] and the references therein.)] On the other hand, in most cases, the current on the cathode of a vacuum arc is localized in bright, narrow regions, or cathode spots. Cathode spots in vacuum arcs have been an object of careful experimental investigations (see [3]–[9] and the references therein). At present, the most important mechanisms dominating the physics of cathode spots are assumed to be bombardment of the cathode surface by ions coming from an "external" plasma (a plasma generated for the arc triggering, a bulk background plasma, or a plasma cloud left over from a previous spot in the immediate vicinity); vaporization of the cathode material in the spot, its subsequent ionization, and the interaction of the produced plasma with the cathode; Joule heating in the cathode body; and motion of the molten metal under the effect of the plasma pressure and the Lorentz force.

Several decades of research have resulted in a variety of approaches available in the literature for modeling cathode spots in vacuum arcs. There are space-resolved descriptions of spots based on a numerical solution of 1-D [10]–[15] and 2-D [16]–[25] differential equations. Many of the available models consider the existence of an external plasma, which provides ions that enter the cathode sheath with the Bohm speed and impinge on the cathode surface. This ion source, with given spatial and temporal distributions, heats the cathode and initiates the spot. The development of the spot is computed with the heat conduction equation, taking into account Joule heating and the energy balance at the cathode surface. In a number of works, such modeling has revealed a fast increase in temperature in a certain region of the cathode body up to values exceeding the critical temperature of the cathode material. This phenomenon may be interpreted as a microexplosion of the cathode and is often called thermal runaway.

Most models neglect the hydrodynamic aspects of the problem, such as motion of the molten metal and convective heat transfer. The exceptions are [18]–[20] and [24]. The models in [19] and [24] employ significantly different approximations and the results differ as well. In [19], the hydrodynamic aspects are considered in a simplified way, on the basis of analysis of the pressure balance at the plasma–cathode interface. A stability criterion determines whether the molten protrusion remains stable or is removed, thus accounting for the change in shape of the cathode surface. No thermal runaway was found; the protrusion is destroyed by melting and under the action of the plasma pressure.

In [24], the hydrodynamic aspects were treated in a more accurate way, on the basis of the Navier–Stokes equations. In contrast, no mechanism of current transfer to the cathode surface was included and the spatial and temporal distributions of the heat flux density to and the plasma pressure on the cathode surface were specified as a part of input.

Manuscript received January 22, 2017; revised March 22, 2017; accepted March 30, 2017. Date of publication May 17, 2017; date of current version August 9, 2017. This work was supported in part by the Fundação para a Ciência e a Tecnologia of Portugal under Grant Pest OE/UID/FIS/50010/2013 and in part by the Siemens AG. *(Corresponding author: Mikhail S. Benilov).*

M. D. Cunha, H. T. C. Kaufmann, and M. S. Benilov are with the Departamento de Física, FCEE, Universidade da Madeira, Largo do Município, 9000 Funchal, Portugal, and also with the Instituto de Plasmas e Fusão Nuclear, IST, Universidade de Lisboa, 1600-276 Lisboa, Portugal (e-mail: benilov@staff.uma.pt).

W. Hartmann and N. Wenzel are with Siemens AG, Corporate Technology, 91058 Erlangen, Germany.

Color versions of one or more of the figures in this paper are available online at http://ieeexplore.ieee.org.

Digital Object Identifier 10.1109/TPS.2017.2697005

The modeling results reveal the formation of a crater with an axially symmetric liquid–metal jet at the periphery, as a result of displacement of the molten material due to the pressure exerted by the plasma over the cathode surface. Depending on the conditions, the jet head can reach the critical temperature. The formation of droplets does not occur in the modeling. The authors supposed that this occurs through a breaking of the axial symmetry of the jet due to the development of a hydrodynamic instability, presumably of the Rayleigh-Plateau type [26]–[28], so its simulation would require 3D modeling which was not attempted in [24].

Note that one of the consequences of current transfer to the cathode surface not being considered in [24] is the neglect of electron emission cooling, which is a strong effect [23], [29] that can significantly affect simulation results. The other consequence is the neglect of the pressure exerted over the cathode surface by ions produced by ionization of the vapor emitted in the spot.

The works [18] and [20] assumed that the most important features of the physics of cathode spots of vacuum arcs are a continuous (without an interface) metal–plasma transition and an explosion-like expansion of the cathode material. A nonstationary two-temperature magnetohydrodynamic model is used with account of ionization kinetics and a wide-range equation of state. Cooling of the cathode due to extraction of the electrons from the metal, which is a strong effect as mentioned above, seems to be neglected. Also neglected are space charge effects.

Thus, although significant advances have been achieved in the last decades, the numerical modeling of cathode spots in vacuum arcs has been inconclusive. The aim of this paper is to perform modeling with account of all of the relevant mechanisms and thus come closer to the understanding of the nature of cathode spots of vacuum arcs. In particular, it will be shown that the effect of the plasma produced by ionization of the metal vapor emitted in the spot indeed significantly affects the development of the spot and the formation of jets and can result in detachment of droplets.

In this paper, the thermal development of a spot is considered, with account of the plasma cloud left over from a previously existing spot, all mechanisms of current transfer to the cathode surface, including the contribution of the plasma produced by ionization of the metal vapor emitted in the spot and the Joule heat generation in the cathode body. The effect of the spatial and temporal distributions of the leftover plasma cloud on spot ignition and development is studied and the temporal evolution of the cathode temperature and of the spot current is analyzed. It is found that in the cases where the spot is ignited, it does not reach steady state; either it explodes (thermal runaway) or is destroyed by thermal conduction after the heating by the leftover plasma cloud has been extinguished. Results of a detailed numerical modeling with account of hydrodynamic processes (convective heat transfer, motion of molten metal, and formation of the crater, liquid–metal jet, and droplets) will be reported in the second part of this paper.

The outline of this paper is as follows. The numerical model is introduced in Section II. The results of simulation are reported and discussed in Section III. Conclusions are summarized in Section IV.

II. Model

The model employed in this paper builds upon a self-consistent space-resolved model of stationary cathode spots in vacuum arcs [23], [30], [31]. It exploits the fact that significant power is deposited into the near-cathode space-charge sheath by the arc power supply. Part of this power is transported from the sheath to the cathode surface and the rest is transported by electric current into the arc column. The latter means that the plasma–cathode interaction to the first approximation is not affected by processes in the arc column. Note that this approach, which is sometimes called the model of nonlinear surface heating, has also been used in the theory and modeling of plasma–cathode interaction in arcs in ambient gases; the recent comparison of models of various levels of complexity of plasma–cathode interaction in atmospheric-pressure arcs [32] has confirmed that the model of nonlinear surface heating, while being the simplest self-consistent approach, is quite accurate.

The thickness of the near-cathode plasma layer is much smaller than the characteristic radius of the spot, and hence current transfer through this layer is locally 1-D. Therefore, the problem of plasma–cathode interaction may be solved in two steps. In the first step, characteristics of the near-cathode plasma layer are evaluated using a 1-D model. In particular, the net densities of the energy flux $q = q(T_w, U)$ and electric current $j = j(T_w, U)$ are found, computed as functions of the local cathode surface temperature T_w and the near-cathode voltage drop U. In the second step, the temperature T and electric potential φ distributions are calculated in the cathode body by means of solving the time-dependent heat conduction equation, written with account of Joule heat generation in the body of the electrode, and the equation of current continuity supplemented with Ohm's law

$$\rho c_p \frac{\partial T}{\partial t} = \nabla \cdot (\kappa \nabla T) + \sigma (\nabla \varphi)^2 \tag{1}$$

$$\nabla \cdot (\sigma \nabla \varphi) = 0. \tag{2}$$

Equations (1) and (2) are solved under the assumption of axial symmetry in cylindrical coordinates (r, z). The material properties, mass density ρ, specific heat c_p, and thermal and electrical conductivities κ and σ, are treated as functions of the local temperature. Boundary conditions on the cathode surface are written in terms of densities of the energy flux, $\kappa(\partial T/\partial n) = q(T_w, U)$, and electric current, $\sigma(\partial \varphi/\partial n) = j(T_w, U)$, from the plasma to the surface, calculated in the previous step, where n is a direction normal to the cathode surface and directed outward. The boundary conditions far away from the spot are $T \to T_\infty$ and $\varphi \to 0$, where T_∞ is a given parameter (the temperature of the cathode far away from the spot).

The model employed in this paper takes into account two contributions to the densities of energy flux q and electric current j from the plasma to the cathode surface, computed independently of each other: the plasma produced from the

metal vapor emitted by the spot and the leftover plasma cloud

$$q = q_1 + q_2, \quad j = j_1 + j_2. \tag{3}$$

Note that this simple superposition neglects a nonlinear interaction between the leftover plasma and the freshly produced vapor from the spot. Contributions $q_1 = q_1(T_w, U)$ and $j_1 = j_1(T_w, U)$ are obtained by means of the model of near-cathode plasma layers in vacuum arcs [31], based on a numerical simulation of the near-cathode space-charge sheath with ionization of atoms emitted by the cathode surface [30]. Note that while electron emission from cathodes of arcs in ambient gas is of thermionic nature and is adequately described by the Richardson–Schottky formula, emission from hot cathodes of vacuum arcs is of thermofield nature and can be adequately described by the Hantzsche fit formula [33] (see also a comparison in [34] and the corrections in [11]). Since, however, this modeling is intended to describe all stages of life of a spot including ones where the cathode is cold, we do not rely on approximate formulas: the code [31] used in this paper employs the Murphy and Good formalism [35]. (More precisely, the electron emission current density is evaluated by means of the method [34] and the effective work function, which governs the emission-related electron energy flux, by means of the fit formulas [36].)

The contribution of the leftover plasma cloud is written as

$$q_2 = q_i^{(\mathrm{cl})} f_1(r)\, f_2(t), \quad j_2 = j_i^{(\mathrm{cl})} f_1(r)\, f_2(t) \tag{4}$$

where $q_i^{(\mathrm{cl})}$ and $j_i^{(\mathrm{cl})}$ are given parameters and $f_1(r)$ and $f_2(t)$ are given functions characterizing the spatial distribution and temporal evolution of the leftover plasma cloud. The spatial distribution is assumed to be Gaussian: $f_1(r) = e^{-(r/a)^2}$, where a is a given parameter characterizing the spatial extension of the cloud. The plasma cloud does not change appreciably in a time interval τ and then decays with a characteristic time constant τ_0

$$f(t) = \begin{cases} 1, & t \leqslant \tau \\ \exp\left(-\left(\frac{t-\tau}{\tau_0}\right)^2\right), & t > \tau \end{cases} \tag{5}$$

where τ and τ_0 are given parameters.

In order to specify the densities of ion current $j_i^{(\mathrm{cl})}$ and energy flux $q_i^{(\mathrm{cl})}$ from the leftover plasma cloud to the cathode surface, we assume that the cold ions enter the near-cathode space-charge sheath with the Bohm speed and are accelerated by the near-cathode voltage drop U. Then

$$j_i^{(\mathrm{cl})} = Z e n_i \sqrt{\frac{kT_e}{m_i}}, \quad q_i^{(\mathrm{cl})} = j_i^{(\mathrm{cl})} U \tag{6}$$

where n_i, T_e, and Z are the ion density, electron temperature, and average ion charge number in the cloud, respectively, e is the electron charge, m_i is the ion mass, and k is the Boltzmann constant.

Contributions $q_1 = q_1(T_w, U)$ and $j_1 = j_1(T_w, U)$ and all the other characteristics of the near-cathode plasma are computed by means of a Fortran code implementing the 1-D model of near-cathode plasma layers in vacuum arcs [31]. The heat conduction and current continuity equations are solved numerically by means of the commercial software COMSOL Multiphysics. The finite-element mesh is strongly nonuniform, in particular in the vicinity of the spot edge, due to a very fast variation of the density of the energy flux coming from the plasma. A free triangular mesh was used, with several successive refinements in the spot region. The boundary conditions far away from the spot are written in the same form as in [23].

Simulation results reported in this paper refer to copper cathodes of two geometries: a planar cathode and a cathode with a Gaussian-shaped microprotrusion of the form $z = h\, e^{-(r/d)^2}$, where h and d are given parameters characterizing, respectively, the height and the radius of the protrusion. The values $h = 1$ μm and $d = 0.8$ μm were assumed. (Note that the radius of the protrusion at $z = 0.1\ h$, given by $r_{\mathrm{prot}} = d\sqrt{\ln 10}$, equals 1.2 μm.)

The thermal and electrical conductivities of copper were the same as in [23]. The specific heat was the same as in [37]. The function $\rho(T)$ was evaluated with the use of experimental data [38] and estimates [39] for the mass density of liquid copper in the temperature ranges $T = 1358$–2450 K and $T = 3000$–7000 K, respectively, and the value of the mass density at the critical point from [40] ($\rho = 2390$ kg/m^3 for $T = 8390$ K).

The near-cathode voltage drop U was set equal to 20V, which corresponds to initiation of spots under conditions of high-current vacuum arcs typical for, e.g., high-power circuit breakers. The values of the ion density $n_i = 10^{26}$ m^{-3}, electron temperature $T_e = 2$ eV, and ion charge $Z = 2$ were assumed as characteristic for the dense plasma left over from a previous spot for copper cathodes (see [41] and the references therein). Note that these parameters result in a value of $q_i^{(\mathrm{cl})}$ of approximately 1.1×10^{12} W/m^2, which is in line with the values considered in [21], [22], [24], and [25]. The characteristic time τ_0 was set equal to 1 ns.

III. Results

The temporal evolution of the maximum temperature $T_{\max}$ in the body of the cathode with the microprotrusion for different values of a and τ is shown in Fig. 1. For $\tau = 10$ ns [Fig. 1(a)], two scenarios are seen depending on the value of a. Scenario 1 occurs in the cases $a = 0.25$ and 0.5 μm: the maximum temperature of the microprotrusion attains a value of about 1300 K for $a = 0.25$ μm and 3100 K for $a = 0.5$ μm, and then abruptly starts decreasing once the leftover plasma cloud is extinguished (i.e., when $t > \tau$). One can say that the spot was not formed in these two cases. In the case $a = 1$ μm, the maximum temperature of the microprotrusion attains a significantly higher value of about 4700 K at $t \approx 10$ ns; however, it also starts decreasing immediately after. It is legitimate to say that the spot was not ignited in this case either.

Scenario 2 occurs in the cases $a = 3$ μm and $a = 5$ μm: the temperature of the cathode does not start decreasing immediately after attaining its maximum value (which happens at approximately 5 ns), but rather stays more or less constant around 4700–4800 K for some time. It is legitimate to say that the spot was ignited and the ignition time is $t_{ig} \approx 5$ ns.

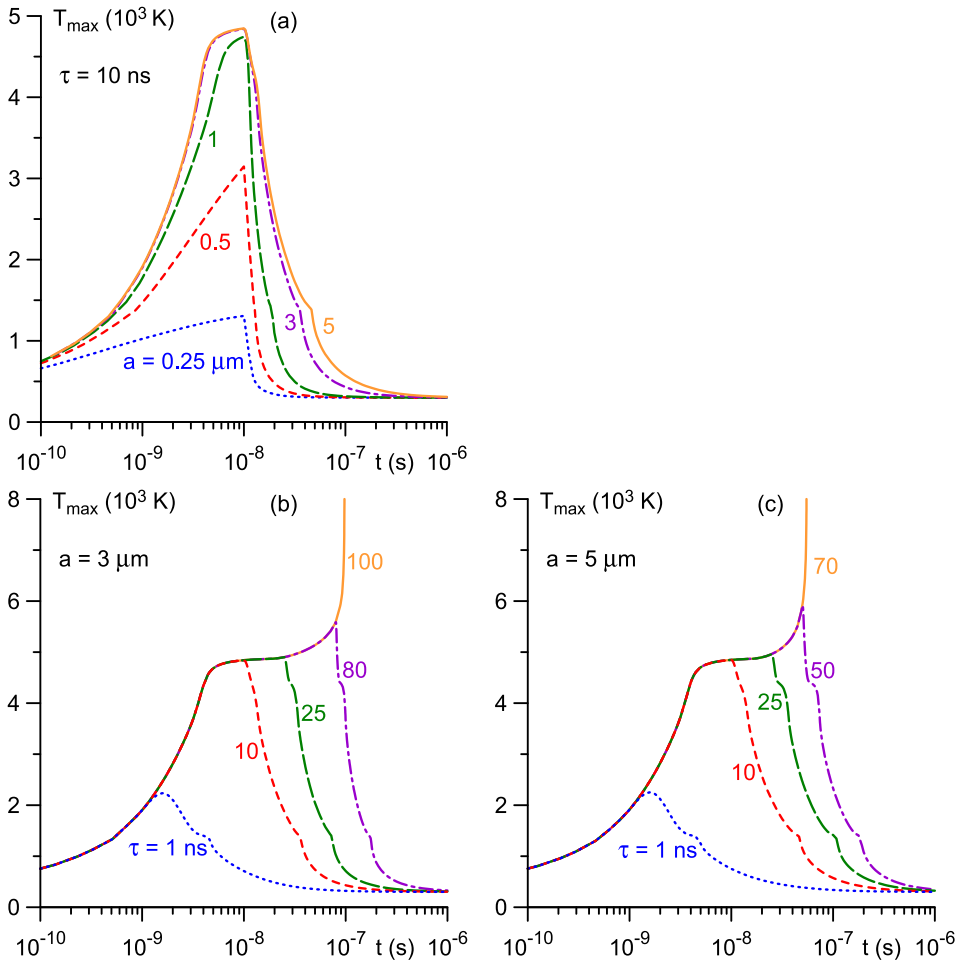

Fig. 1. Temporal evolution of the maximum temperature in the cathode with the microprotrusion.

The similarity of the temporal evolution of $T_{\max}$ in these two cases is understandable since the spatial extension of the leftover plasma cloud exceeds the protrusion radius r_{prot} in both cases. In all the cases, $T_{\max}$ for $t \gtrsim 100$ ns is close to 300 K: the energy supplied by the leftover plasma cloud has been removed by thermal conduction into the bulk of the cathode.

The cases $a = 3$ μm and $a = 5$ μm for τ exceeding 10 ns should be studied in order to identify conditions where $T_{\max}$ reaches the critical temperature of copper, which is 8390 K, i.e., thermal explosion (thermal runaway) occurs. The corresponding plots are shown in Fig. 1(b) and (c). The results for $\tau = 1$ ns are also shown for comparison. The above-described scenario 1 occurs for $\tau = 1$ ns: for both cases $a = 3$ μm [Fig. 1(b)] and $a = 5$ μm [Fig. 1(c)], the temperature of the microprotrusion attains a value of about 2200 K at approximately 1.6 ns and then starts decreasing. The spot was not ignited.

The above-described scenario 2, occurs for $\tau = 10$ ns and $\tau = 25$ ns for both cases $a = 3$ μm and $a = 5$ μm: the spot was ignited and subsequently destroyed by heat removal into the bulk of the cathode due to thermal conduction once the leftover plasma cloud has been extinguished.

Two further scenarios are seen in Fig. 1(b) and (c). Scenario 3 occurs for $\tau = 80$ ns for the case $a = 3$ μm and for $\tau = 50$ ns for the case $a = 5$ μm: the thermal explosion starts developing, with $T_{\max}$ shifting from the surface into the bulk of the protrusion and reaching 5000–6000 K, but then it is quenched by heat conduction once $t > \tau$ and the leftover plasma cloud has been extinguished.

Scenario 4 represents the thermal explosion of the spot. The explosion occurs at $t \approx 97$ ns for the case $a = 3$ μm and at $t \approx 55$ ns for $a = 5$ μm. The evolution of the cathode temperature distribution for the latter case is shown in Fig. 2.

Let us proceed to modeling results for the planar cathode. For brevity, we skip the analog of Fig. 1(a) and note only that the minimum value of the cloud dimension needed for ignition of the spot is $a = 3$ μm and the ignition time is $t_{ig} \approx 8$ ns. The temporal evolution of the maximum temperature $T_{\max}$ in the body of the planar cathode for two values of a and different τ values is shown in Fig. 3. The same four scenarios as above may be identified, although the ignition of the spot and its subsequent explosion develop somewhat slower. Scenario 1 occurs for $\tau = 1$ ns in both cases $a = 5$ μm [Fig. 3(a)] and $a = 10$ μm [Fig. 3(b)]: the cathode temperature reaches a maximum of 1500 K at $t \approx 1.5$ ns and immediately starts decreasing. Scenario 2 (formation of a transient spot eventually

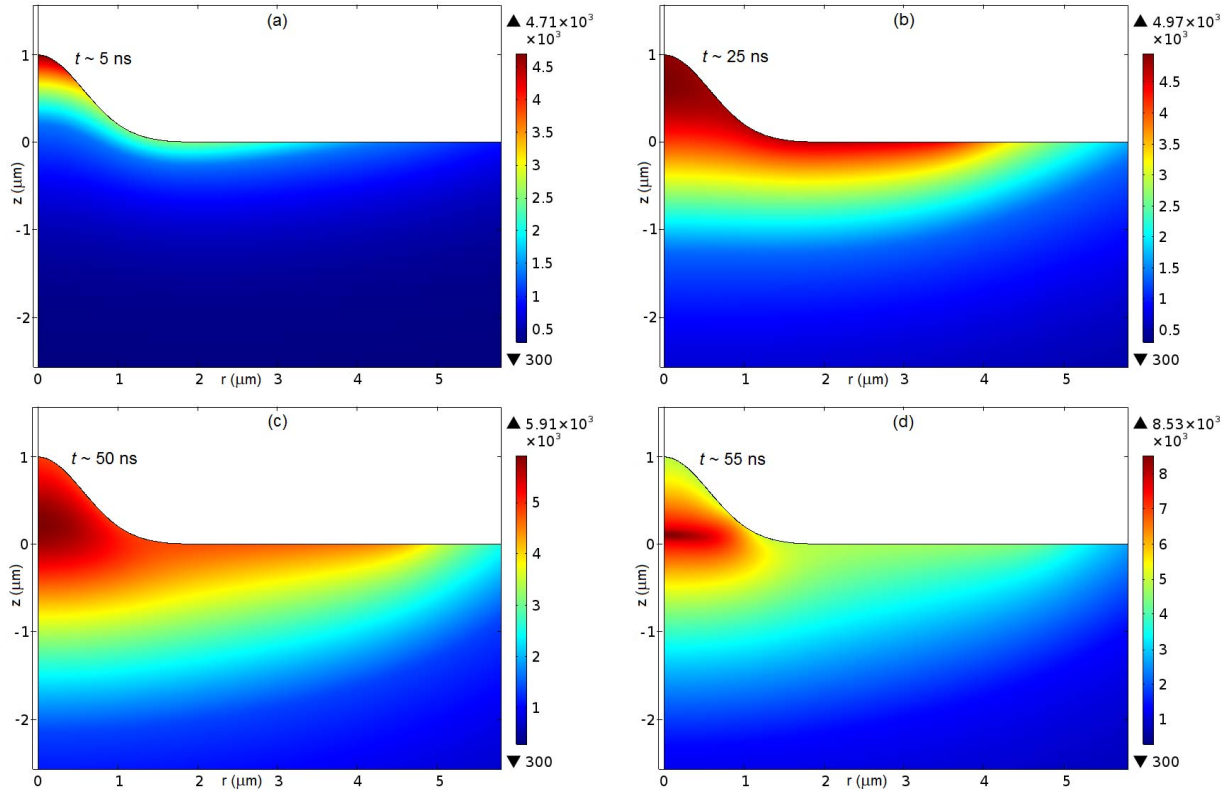

Fig. 2. Evolution of temperature distribution in the cathode with the microprotrusion. $a = 5$ μm and $\tau = 70$ ns. The bar in kelvin.

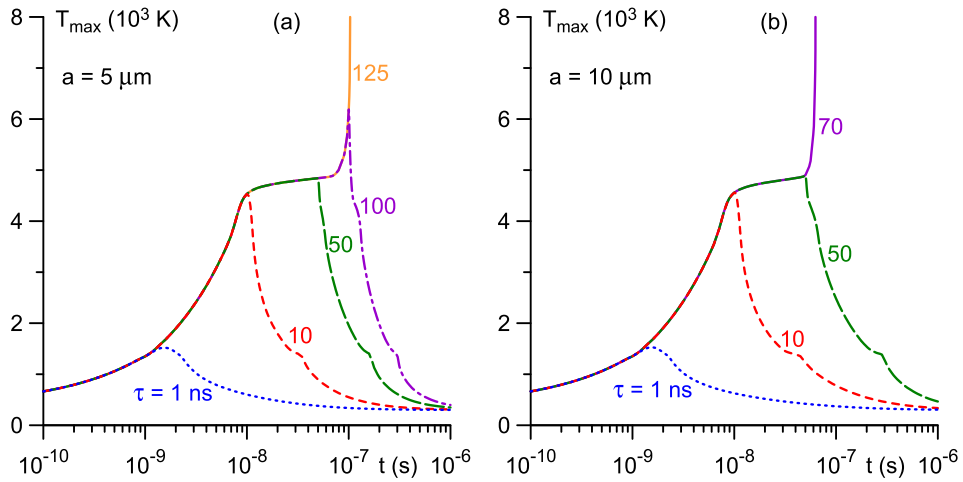

Fig. 3. Temporal evolution of the maximum temperature in the planar cathode.

destroyed by heat removal into the bulk of the cathode due to thermal conduction) occurs for $\tau = 10$ ns and $\tau = 50$ ns for both cases $a = 5$ μm and $a = 10$ μm, with ignition of the spot at $t_{ig} \approx 8$ ns. Thermal runaway is initiated but then quenched by thermal conduction (scenario 3) for the case $a = 5$ μm for $\tau = 100$ ns. Lastly, the thermal explosion (scenario 4) occurs at $t \approx 103$ ns for $a = 5$ μm and at $t \approx 63$ ns for $a = 10$ μm. Similar to the case of the microprotrusion, the maximum temperature in the spot is more or less constant after the spot has been ignited, until either the extinction of the leftover plasma cloud (scenario 2) or the beginning of thermal runaway (scenarios 3 and 4). The evolution of the cathode temperature distribution for scenario 4 in the case $a = 5$ μm is shown in Fig. 4.

Thus, in both cases of the cathode with the protrusion and the planar cathode, there is a plateau in the temporal evolution of the spot temperature after the ignition and before the plasma cloud has been extinguished or thermal runaway develops, whichever happens earlier. This remarkable feature is known from the modeling of cathode spots in arcs in high-pressure ambient gases [29] and may be understood as follows. As the cathode surface temperature T_w increases

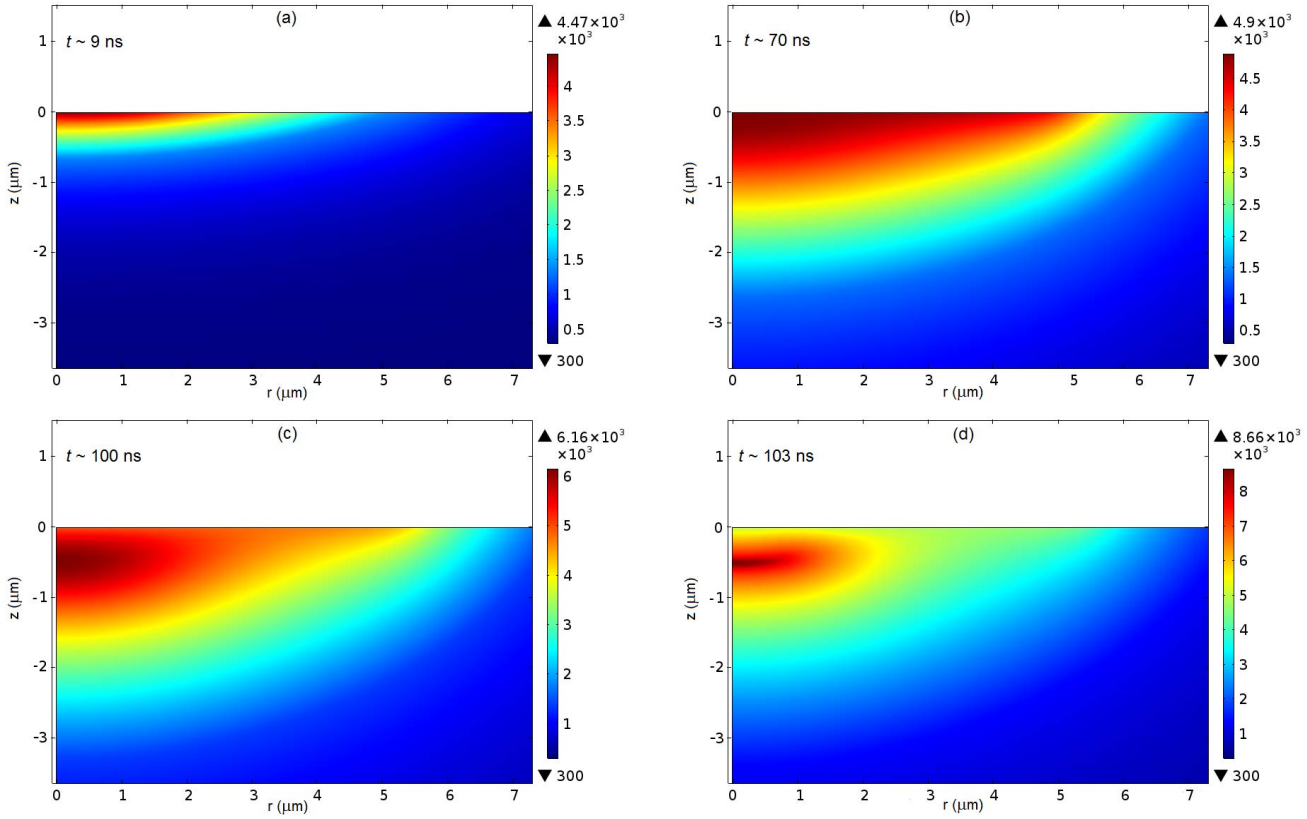

Fig. 4. Evolution of temperature distribution in the planar cathode. $a = 5$ μm and $\tau = 125$ ns. The bar in kelvin.

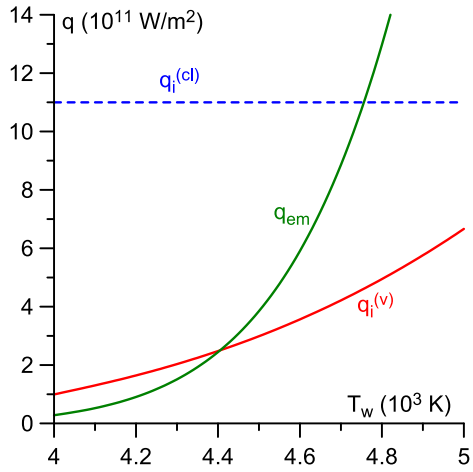

Fig. 5. q_{em}: energy removed from the cathode surface due to electron emission. $q_i^{(v)}$ and $q_i^{(\mathrm{cl})}$: energies delivered to the cathode surface by the ions produced by ionization of the vapor emitted in the spot and by the ions from the leftover plasma cloud, respectively.

with time, so do the different contributions to the density $q_1 = q_1(T_w, U)$ of the energy flux from the plasma produced by ionization of the emitted vapor in the cathode spot. The most relevant contributions to q_1 are the heating by incident ions produced by ionization of the vapor $q_i^{(v)}$ and the cooling by the electron emission q_{em}. Their dependence on the cathode surface temperature T_w is shown in Fig. 5. Also shown in Fig. 5 is $q_i^{(\mathrm{cl})}$, the heating by the leftover plasma cloud. The combined ion heating $q_i^{(v)} + q_i^{(\mathrm{cl})}$ exceeds q_{em} for T_w below approximately 4700 K. It is intuitively clear that 4700–4800 K represents the upper limit of the cathode temperature until the Joule heating comes into play and thermal runaway starts developing. (In mathematical terms, this is a corollary of the maximum principle for harmonic functions [29].) Note that while $q_i^{(v)}$ is smaller (by approximately a factor of 3) than $q_i^{(\mathrm{cl})}$ at such temperatures, its contribution to the surface heating is nevertheless appreciable.

Since the spot temperature does not change much after ignition and before the plasma cloud has been extinguished or thermal runaway develops, plasma parameters inside the spot, including the current density, also experience little variation. One can say that the "spot brightness" remains approximately constant. On the other hand, the spot significantly expands, as is illustrated in Fig. 2(a) and (b) for the cathode with the protrusion and Fig. 4(a) and (b) for the planar cathode.

The model being used allows one to self-consistently evaluate various spot parameters, including the current I. The temporal evolution of the current during the spot ignition and development is shown for the case $a = 5$ μm for the cathode with the microprotrusion [Fig. 6(a)] and for the planar cathode [Fig. 6(b)]. One can identify the moment of ignition of the spot, $t_{ig} \approx 5$ ns for the cathode with the protrusion and $t_{ig} \approx 8$ ns for the planar cathode, as the instant when the current starts increasing from the constant value of current supplied by the leftover plasma cloud (approximately 4.4A). This coincides with the maximum temperature in the cathode attaining a value around 4700–4800 K [see Figs. 1(c) and 3(a)].

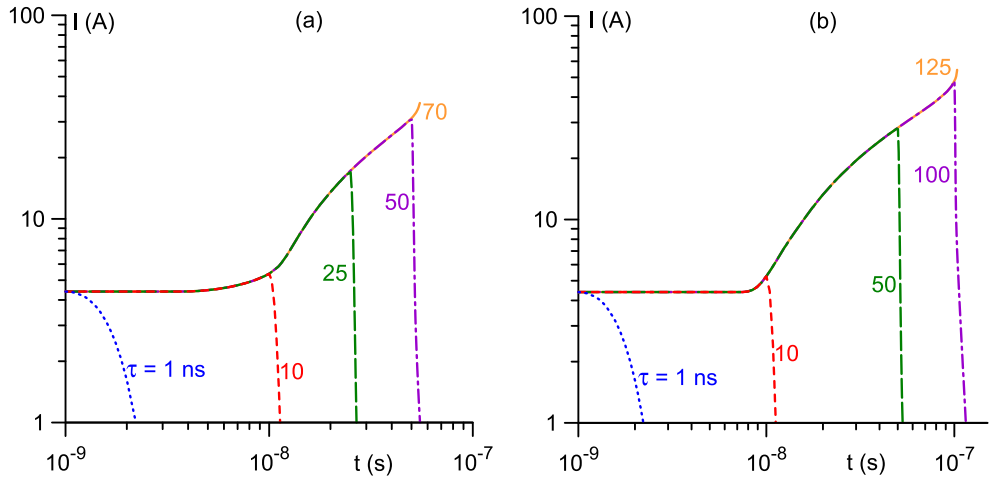

Fig. 6. Evolution of spot current. (a) Cathode with the microprotrusion. (b) Planar cathode. $a = 5\ \mu$m.

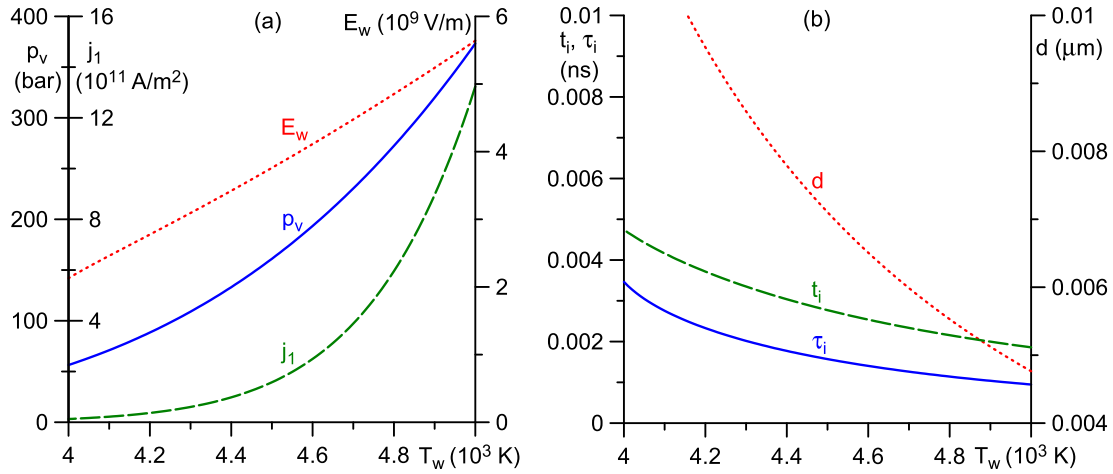

Fig. 7. Parameters of the near-cathode plasma layer inside the spot. p_v: saturated vapor pressure. j_1: density of electric current to the cathode surface due to plasma produced from the metal vapor emitted by the spot. E_w: electric field at the cathode surface. t_i: time of flight of the ions across the sheath. τ_i: time scale of ionization of the emitted vapor atoms. d: sheath thickness.

However, the plateau visible in the evolution of $T_{\max}$ is absent in the evolution of I: the current continually increases from the moment of spot ignition until the explosion or the extinction of the leftover plasma cloud. Since there is little variation in the spot temperature after the spot has been ignited, and therefore, in the current density inside the spot, the rise in current is due to the expansion of the spot over the cathode surface seen in Figs. 2(a) and (b) and 4(a) and (b).

It is of interest to also consider the parameters of the near-cathode plasma layer inside the spot. Several such parameters evaluated by means of the model [31] are shown in Fig. 7 in the relevant range of the cathode surface temperatures. The saturated vapor pressure p_v, the electric field E_w at the cathode surface, and the current density $j_1 = j_1(T_w, U)$ are shown in Fig. 7(a); note that p_v governs the density of flux of vaporized atoms by means of the Langmuir formula: $J_v = p_v/(2\pi m_i k T_w)^{1/2}$. Since E_w exceeds 10^9V/m, the electron emission is not of thermionic nature, in agreement with what was expected. Note that the emission-related electron energy flux is always directed into the plasma in the conditions of Fig. 7(a), i.e., electron emission contributes to cooling of the cathode.

Other parameters of interest are the sheath thickness d, the time of flight of the ions across the sheath t_i, and the time scale τ_i of ionization of the emitted vapor atoms. Although the asymptotic sheath theory [30], which is the basis of the code [31] used in this modeling, does not involve any (finite) sheath thickness, representative values of d may be obtained by means of the Child–Langmuir sheath model evaluated in terms of ion current density and sheath voltage. The time of flight of the ions across the Child–Langmuir sheath evaluated for copper ions for the sheath voltage of 20 V may be written as 0.39 $(d/\mu m)$ ns. In the framework of the asymptotic sheath theory [30], the time scale of ionization of the emitted vapor atoms may be estimated as $\tau_i = 1/k_i n_a^{(0)}$, where k_i is the rate constant of ionization by electron impact and $n_a^{(0)}$ is the value of the atomic density at the point of maximum of electrostatic potential. For the purposes of evaluation, this expression may be rewritten as $\tau_i = N_{\rm aw}/k_i n_{\rm aw}$, where $n_{\rm aw}$ is the value of atomic density at the cathode surface evaluated as described

in [31] and N_{aw} is given by [31, eq. (3)]. The parameters d, t_i, and τ_i evaluated in this way are shown in Fig. 7(b).

The assumption of a 1-D quasi-stationary near-cathode layer [30], [31] requires that the sheath thickness d be much smaller than the transversal dimensions (the spot radius and dimensions of protrusions) and that τ_i and t_i be much smaller than the characteristic time scales of development of the spot. Given the representative values shown in Fig. 7(b), these requirements are met with a large margin.

IV. Conclusion

The developed model describes the initiation and development of a cathode spot in a high-current vacuum arc, with account of the plasma cloud left over from a previously existing spot or generated at arc triggering, all the mechanisms of current transfer to the cathode surface, and the Joule heat generation in the cathode body.

The account of all the mechanisms of current transfer, including the contributions from both the leftover plasma cloud and the plasma produced by ionization of the metal vapor emitted in the spot, allows one to identify in a natural way the different phases of life of an individual cathode spot: the ignition, the expansion over the cathode surface, and the thermal explosion or destruction by heat removal into the bulk of the cathode due to thermal conduction. The states shown in Figs. 2(a) and 4(a) exemplify the end of the ignition phase; the expansion phase occurs between the states in Figs. 2(a) and (b), and 4(a) and (b), and the states in Figs. 2(b)-(d) and 4(b)-(d) exemplify the thermal runaway development.

The ignition phase is characterized by a fast increase in the temperature of the cathode surface under the effect of the ions coming from the leftover plasma. In the conditions of Figs. 1(c) and 3(a), this phase terminates at approximately 5 or 8 ns, respectively. In Fig. 6, this phase is associated with the horizontal section of the dependence $I(t)$.

After the spot has been ignited, the maximum temperature of the cathode, which occurs at the surface, does not change much and is approximately 4700–4800 K. This is the surface temperature at which the heating of the cathode surface, which is due to bombardment by the ions originating in the leftover plasma cloud and by the ions produced in the ionization of atoms vaporized from the surface, is balanced by the cooling of the cathode surface, which is due to electron emission. This remarkable feature is known from the modeling of cathode spots in arcs in high-pressure ambient gases and manifests itself as the plateau in the dependence $T_{max}(t)$ seen in Figs. 1(b) and (c) and 3. One can say that the spot brightness does not change much during this phase. However, this does not mean that the spot has reached a steady state: the spot expands over the cathode surface, so the spot current increases.

Eventually, the maximum of the cathode temperature is shifted from the surface into the cathode: the Joule heating comes into play and thermal runaway starts developing below the cathode surface, leading to an explosion (thermal runaway). The explosion can occur not only on a cathode with a microprotrusion but also on a planar cathode.

The development of the spot is interrupted if the leftover plasma cloud has been extinguished: the spot is destroyed by heat removal into the bulk of the cathode due to thermal conduction. Therefore, different scenarios are possible depending on the time of action of the cloud: the spot may be quenched before having been formed or during the expansion phase, or even at the initial stage of thermal explosion. It should be stressed that parameters of the plasma cloud required for the ignition, and eventual explosion, of the spot on the cathode with a 1-μm-scale microprotrusion and on the planar cathode are of the same order of magnitude. Indeed, the minimum spatial extension and the time of action of the leftover plasma cloud needed for the spot to be ignited are $a = 3$ μm and $t_{ig} = 5$ ns for the cathode with the microprotrusion and $a = 3$ μm and $t_{ig} = 8$ ns for the planar cathode, respectively; the time of action needed for the explosion for $a = 5$ μm is 55 ns for the cathode with the microprotrusion and 103 ns for the planar cathode. Also of the same order are the total energies that need to be deposited by the leftover plasma cloud for the spot to be ignited and eventually exploded, $Q = \pi a^2 q_i^{(cl)} t$; for example, the energy required for ignition (with $a = 3$ μm) is 0.16 μJ for the cathode with the microprotrusion and 0.25 μJ for the planar cathode.

In all the cases where the spot is ignited, it either explodes or is destroyed by thermal conduction; a steady state is never reached. This is consistent with the results of investigation of stability of stationary cathode spots of vacuum arcs [37]: the spots operating at a fixed value of the near-cathode voltage are unstable.

Results of simulations with account of motion of the molten metal, convective heat transfer, and surface deformation will be reported in the second part of this paper. Here, we indicate only the following. The account of the hydrodynamic aspects does not affect the main features of development of the cathode spot reported in this paper: the above-described ignition and expansion phases remain clearly identifiable; the plateau in the cathode temperature evolution during the expansion phase remains present; the destruction of the spot by thermal conduction (accompanied by solidification of the molten metal) occurs after the leftover plasma cloud has been extinguished. Furthermore, the motion of the molten metal comes into play on a time scale longer than the spot ignition times, and hence results on the spot ignition time and the initial stage of the expansion phase, computed in this paper, remain applicable. As the spot expands further, the hydrodynamic effects come into play and, in particular, suppress the development of thermal runaway and may cause detachment of droplets.

An important question is if parameters of the near-cathode plasma remaining after the spot extinction are sufficient to initiate a new spot. This question needs to be considered with account of the hydrodynamic aspects and is therefore beyond the scope of this paper. Relevant estimates will be given in the second part of this paper.

References

[1] R. Kh Amirov *et al.*, "Vacuum arc with a distributed cathode spot as a plasma source for plasma separation of spent nuclear fuel and radioactive waste," *Plasma Phys. Rep.*, vol. 41, no. 10, pp. 808–813, 2015. [Online]. Available: http://dx.doi.org/10.1134/S1063780X15100013

[2] M. S. Benilov and L. G. Benilova, "Physics of spotless mode of current transfer to cathodes of metal vapor arcs," *IEEE Trans. Plasma Sci.*, vol. 43, no. 8, pp. 2247–2252, Oct. 2015. [Online]. Available: http://dx.doi.org/10.1109/TPS.2015.2445093

[3] V. F. Puchkarev, "Cathode spots (chapter summary)," in *Handbook of Vacuum Arc Science and Technology: Fundamentals and Applications*, R. L. Boxman, D. M. Sanders, and P. J. Martin, Eds. Park Ridge, NJ, USA: Noyes Publications, 1995, pp. 256–264.

[4] B. Jüttner, "Cathode spots of electric arcs," *J. Phys. D, Appl. Phys.*, vol. 34, no. 17, pp. R103–123, 2001. [Online]. Available: http://iopscience.iop.org/0022-3727/34/17/202

[5] A. Batrakov, S. Popov, N. Vogel, B. Juttner, and D. Proskurovsky, "Plasma parameters of an arc cathode spot at the low-current vacuum discharge," *IEEE Trans. Plasma Sci.*, vol. 31, no. 5, pp. 817–821, Oct. 2003.

[6] A. Anders, E. M. Oks, G. Y. Yushkov, K. P. Savkin, I. G. Brown, and A. G. Nikolaev, "Measurements of the total ion flux from vacuum arc cathode spots," *IEEE Trans. Plasma Sci.*, vol. 33, no. 5, pp. 1532–1536, May 2005.

[7] A. Anders, *Cathodic Arcs: From Fractal Spots to Energetic Condensation* (Springer Series on Atomic, Optical, and Plasma Physics). New York, NY, USA: Springer, 2008.

[8] A. M. Chaly and S. M. Shkol'nik, "Low-current vacuum arcs with short arc length in magnetic fields of different orientations: A review," *IEEE Trans. Plasma Sci.*, vol. 39, no. 6, pp. 1311–1318, Jun. 2011.

[9] S. Jia, Z. Shi, and L. Wang, "Vacuum arc under axial magnetic fields: Experimental and simulation research," *J. Phys. D, Appl. Phys.*, vol. 47, p. 403001, Sep. 2014. [Online]. Available: http://dx.doi.org/10.1088/0022-3727/47/40/403001

[10] J. Prock, "Time-dependent description of cathode crater formation in vacuum arcs," *IEEE Trans. Plasma Sci.*, vol. 14, no. 4, pp. 482–491, Aug. 1986. [Online]. Available: http://ieeexplore.ieee.org/stamp/stamp.jsp?tp=&arnumber=4316578

[11] J. Mitterauer and P. Till, "Computer simulation of the dynamics of plasma-surface interactions in vacuum arc cathode spots," *IEEE Trans. Plasma Sci.*, vol. 15, no. 5, pp. 488–501, Oct. 1987. [Online]. Available: http://ieeexplore.ieee.org/stamp/stamp.jsp?tp=&arnumber=4316742

[12] T. Klein, J. Paulini, and G. Simon, "Time-resolved description of cathode spot development in vacuum arcs," *J. Phys. D, Appl. Phys.*, vol. 27, no. 9, p. 1914, 1994. [Online]. Available: http://stacks.iop.org/0022-3727/27/i=9/a=015

[13] I. I. Beilis, "The nature of high voltage initiation of an electrical arc in a vacuum," *Appl. Phys. Lett.*, vol. 97, no. 12, p. 121501, 2010. [Online]. Available: http://link.aip.org/link/?APL/97/121501/1

[14] I. I. Beilis, "Cathode spot development on a bulk cathode in a vacuum arc," *IEEE Trans. Plasma Sci.*, vol. 41, no. 8, pp. 1979–1986, Aug. 2013.

[15] D. L. Shmelev and S. A. Barengolts, "Kinetic modeling of initiation of explosion center on cathode under dense plasma," *IEEE Trans. Plasma Sci.*, vol. 41, pp. 1959–1963, 2013.

[16] M. S. Benilov, "Nonlinear heat structures and arc-discharge electrode spots," *Phys. Rev. E, Stat. Phys. Plasmas Fluids Relat. Interdiscip. Top.*, vol. 48, no. 1, pp. 506–515, 1993. [Online]. Available: http://pre.aps.org/abstract/PRE/v48/i1/p506_1

[17] Z.-J. He and R. Haug, "Cathode spot initiation in different external conditions," *J. Phys. D, Appl. Phys.*, vol. 30, no. 4, pp. 603–613, 1997. [Online]. Available: http://stacks.iop.org/0022-3727/30/603

[18] D. L. Shmelev and E. A. Litvinov, "The computer simulation of the vacuum arc emission center," *IEEE Trans. Plasma Sci.*, vol. 25, no. 4, pp. 533–537, Aug. 1997. [Online]. Available: http://ieeexplore.ieee.org/xpl/articleDetails.jsp?arnumber=640661

[19] R. Schmoll, "Analysis of the interaction of cathode microprotrusions with low-temperature plasmas," *J. Phys. D, Appl. Phys.*, vol. 31, no. 15, p. 1841, 1998. [Online]. Available: http://stacks.iop.org/0022-3727/31/i=15/a=012

[20] D. L. Shmelev and E. A. Litvinov, "Computer simulation of ecton in a vacuum arc," *IEEE Trans. Dielectr. Electr. Insul.*, vol. 6, no. 4, pp. 441–444, Aug. 1999. [Online]. Available: http://ieeexplore.ieee.org/xpl/articleDetails.jsp?arnumber=788741

[21] I. V. Uimanov, "A two-dimensional nonstationary model of the initiation of an explosive center beneath the plasma of a vacuum arc cathode spot," *IEEE Trans. Plasma Sci.*, vol. 31, no. 5, pp. 822–826, Oct. 2003.

[22] S. A. Barengolts, G. A. Mesyats, and M. M. Tsventoukh, "Initiation of ecton processes by interaction of a plasma with a microprotrusion on a metal surface," *J. Experim. Theor. Phys.*, vol. 107, no. 6, pp. 1039–1048, 2008. [Online]. Available: http://dx.doi.org/10.1134/S1063776108120133

[23] M. S. Benilov, M. D. Cunha, W. Hartmann, S. Kosse, A. Lawall, and N. Wenzel, "Space-resolved modeling of stationary spots on copper vacuum arc cathodes and on composite CuCr cathodes with large grains," *IEEE Trans. Plasma Sci.*, vol. 41, no. 8, pp. 1950–1958, Oct. 2013. [Online]. Available: http://dx.doi.org/10.1109/TPS.2013.2263255

[24] G. A. Mesyats and I. V. Uimanov, "Hydrodynamics of the molten metal during the crater formation on the cathode surface in a vacuum arc," *IEEE Trans. Plasma Sci.*, vol. 43, no. 8, pp. 2241–2246, Aug. 2015.

[25] S. A. Barengolts, D. L. Shmelev, and I. V. Uimanov, "Pre-explosion phenomena beneath the plasma of a vacuum arc cathode spot," *IEEE Trans. Plasma Sci.*, vol. 43, no. 8, pp. 2236–2240, Sep. 2015.

[26] G. A. Mesyats and N. M. Zubarev, "The Rayleigh–Plateau instability and jet formation during the extrusion of liquid metal from craters in a vacuum arc cathode spot," *J. Appl. Phys.*, vol. 117, no. 4, p. 043302, 2015. [Online]. Available: http://scitation.aip.org/content/aip/journal/jap/117/4/10.1063/1.4906559

[27] M. A. Gashkov, N. M. Zubarev, O. V. Zubareva, G. A. Mesyats, and I. V. Uimanov, "Model of liquid-metal splashing in the cathode spot of a vacuum arc discharge," *J. Experim. Theor. Phys.*, vol. 122, no. 4, pp. 776–786, 2016.

[28] M. A. Gashkov, N. M. Zubarev, G. A. Mesyats, and I. V. Uimanov, "The mechanism of liquid metal jet formation in the cathode spot of vacuum arc discharge," *Tech. Phys. Lett.*, vol. 42, no. 8, pp. 852–855, 2016.

[29] M. S. Benilov and M. D. Cunha, "Heating of refractory cathodes by high-pressure arc plasmas: II," *J. Phys. D, Appl. Phys.*, vol. 36, no. 6, pp. 603–614, 2003. [Online]. Available: http://stacks.iop.org/0022-3727/36/i=6/a=301

[30] M. S. Benilov and L. G. Benilova, "The double sheath on cathodes of discharges burning in cathode vapour," *J. Phys. D, Appl. Phys.*, vol. 43, no. 34, p. 345204, 2010. [Online]. Available: http://stacks.iop.org/0022-3727/43/i=34/a=345204

[31] N. A. Almeida, M. S. Benilov, L. G. Benilova, W. Hartmann, and N. Wenzel, "Near-cathode plasma layer on CuCr contacts of vacuum arcs," *IEEE Trans. Plasma Sci.*, vol. 41, no. 8, pp. 1938–1949, Apr. 2013. [Online]. Available: http://dx.doi.org/10.1109/TPS.2013.2260832

[32] M. S. Benilov, N. A. Almeida, M. Baeva, M. D. Cunha, L. G. Benilova, and D. Uhrlandt, "Account of near-cathode sheath in numerical models of high-pressure arc discharges," *J. Phys. D, Appl. Phys.*, vol. 49, no. 21, p. 215201, 2016. [Online]. Available: http://stacks.iop.org/0022-3727/49/i=21/a=215201

[33] E. Hantzsche, "The thermo-field emission of electrons in arc discharges," *Beitr. Plasmaphys.*, vol. 22, no. 4, pp. 325–346, 1982. [Online]. Available: http://dx.doi.org/10.1002/ctpp.19820220403

[34] M. S. Benilov and L. G. Benilova, "Field to thermo-field to thermionic electron emission: A practical guide to evaluation and electron emission from arc cathodes," *J. Appl. Phys.*, vol. 114, no. 6, p. 063307, 2013. [Online]. Available: http://link.aip.org/link/?JAP/114/063307/1

[35] E. L. Murphy and R. H. Good, "Thermionic emission, field emission, and the transition region," *Phys. Rev.*, vol. 102, no. 6, pp. 1464–1473, 1956. [Online]. Available: http://link.aps.org/doi/10.1103/PhysRev.102.1464

[36] J. Paulini, T. Klein, and G. Simon, "Thermo-field emission and the Nottingham effect," *J. Phys. D, Appl. Phys.*, vol. 26, no. 8, pp. 1310–1315, 1993. [Online]. Available: http://stacks.iop.org/0022-3727/26/1310

[37] M. S. Benilov, M. D. Cunha, W. Hartmann, and N. Wenzel, "Numerical investigation of the stability of stationary solutions in the theory of cathode spots in arcs in vacuum and ambient gas," *Plasma Sour. Sci. Technol.*, vol. 23, no. 5, p. 054007, 2014. [Online]. Available: http://stacks.iop.org/0963-0252/23/i=5/a=054007

[38] M. J. Assael *et al.*, "Reference data for the density and viscosity of liquid copper and liquid tin," *J. Phys. Chem. Reference Data*, vol. 39, no. 3, p. 033105, 2010. [Online]. Available: http://scitation.aip.org/content/aip/journal/jpcrd/39/3/10.1063/1.3467496

[39] J. A. Cahill and A. D. Kirshenbaum, "The density of liquid copper from its melting point (1356k) to 2500k and an estimate of its critical constants," *J. Phys. Chem.*, vol. 66, no. 6, p. 1080, 1962.

[40] V. E. Fortov, I. T. Iakubov, and A. G. Khrapak, *Physics of Strongly Coupled Plasma*. Oxford, U.K.: Oxford Univ. Press, 2007.

[41] G. A. Mesyats and S. A. Barengol'ts, "Generation mechanism of anomalous ions in vacuum arcs," *Phys. Uspekhi*, vol. 45, no. 10, pp. 1001–1018, 2002. [Online]. Available: http://iopscience.iop.org/1063-7869/45/10/R01

Mário D. Cunha received the Ph.D. degree in physics from the University of Madeira, Madeira, Portugal, in 2004. His thesis focused on the modeling of the plasma-cathode interaction in high-pressure arc discharges.

He is currently an Assistant Professor with the Department of Physics, University of Madeira. His current research interests include numerical simulation of different modes of current transfer to cathodes of high-pressure arc discharges, and also spots on vacuum arc cathodes.

Helena T. C. Kaufmann received the M.Sci. degree (incorporating bachelor's level study) in physics from the Imperial College of Science, Technology and Medicine, London, U.K., in 2012. She is currently pursuing the Ph.D. degree in physics with the Department of Physics, University of Madeira, Madeira, Portugal.

She was involved in the plasma-cathode interaction in vacuum arcs, in particular, the numerical modeling of spots on vacuum arc cathodes.

Mikhail S. Benilov received the Diploma degree (Hons.) and the C.Sc. (Ph.D.) degree in physics from the Moscow Institute for Physics and Technology, Moscow, Russia, in 1974 and 1978, respectively, and the Ph.D. degree in physical and mathematical sciences from the Institute for High Temperatures, USSR Academy of Sciences, Moscow, in 1990. His thesis focused on the theory of electrostatic probes and electrodes in high-pressure flowing plasmas.

He was with the Institute for High Temperatures, where he led a group involved in plasma and nonlinear physics, numerical modeling, and fluid dynamics, after completing postgraduate courses with the Moscow Institute for Physics and Technology and the Institute for Mechanics, Lomonosov Moscow State University, Moscow, in 1977. Since 1993, he has been a Professor with the Department of Physics, University of Madeira. His current research interests include plasma physics, in particular, plasma-electrode interaction, nonlinear physics, and numerical modeling.

Dr. Benilov was a recipient of the Alexander von Humboldt Research Fellowship in 1990 and stayed for two years with Ruhr-Universität Bochum, Germany, where he was involved in the theory and simulation of near-electrode phenomena.

Werner Hartmann received the M.S. degree in physics and the Ph.D. degree from the University of Erlangen, Erlangen, Germany, in 1981 and 1986, respectively.

He was a Research and Teaching Assistant with the Physics Department, University of Erlangen, from 1986 to 1991, and with the University of Southern California, Los Angeles, CA, USA, in 1987 and 1988, where he conducted research on cold cathode thyratrons/pseudosparks and fast dynamic z-pinches as extreme ultraviolet light sources. He was responsible for fundamental and applied research into vacuum switching arc physics and devices at the Siemens Corporate Technology, Erlangen, Germany, being involved in the development of low-voltage contactors, low-voltage circuit breakers up to 130-kA breaking capacity, medium voltage vacuum circuit breakers, and the successful development of high voltage vacuum circuit breakers for 72 and 145 kV. He was involved in the development of a fully 3-D, fully transient software code for the simulation of low-voltage switching arcs in air as a Project Manager. He developed environmental and environmentally friendly technologies for industrial applications, mainly in the areas of clean water, clean air, and electroporation. He has been a Researcher, a Research Group Leader, a Project Manager, and a Program Manager with Siemens Corporate Technology, since 1991.

Currently, he holds the position of a Senior Key Expert in the area of environmental technologies. His current research interests include the field of mining applications, particularly in the field of flotation and magnetic separation.

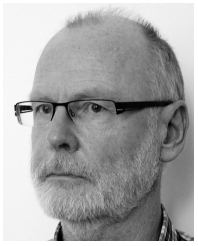

Norbert Wenzel received the M.Ed. degree in physics and mathematics and the Ph.D. degree in physics from the University of Heidelberg, Heidelberg, Germany, in 1979 and 1985, respectively.

From 1978 to 1985, he was a Research and Teaching Assistant with the Applied Physics Department, University of Heidelberg, and the Plasma Research Institute, University of Stuttgart, Stuttgart, Germany, with a focus on fusion-oriented plasma physics and plasma diagnostics. In 1982, he held a EURATOM fellowship at the Nuclear Fusion Research Center, Association ENEA, Frascati, Italy. From 1985 to 1992, he applied nonlinear Raman spectroscopy to industrial processes, such as low voltage air breakers and gas lasers. He developed sealed-off carbon dioxide slab lasers excited by radio-waves and microwaves. Since 1985, he has been a Researcher, a Test Laboratory Head, a Project Leader, and a Radiation Protection Officer with Siemens Corporate Technology, where he has been in the field of fundamental and applied research of switching arcs since 1992. As the Head of a synthetic test laboratory, he was involved in the development of low, medium, and high voltage vacuum interrupters. Since 2006, he has been extending his activities to physical modeling and numerical simulation of vacuum arc plasmas taking into account cathode surface phenomena. He currently holds the position of a Senior Key Expert Research Scientist in the area of vacuum switching technologies.